

# A biodegradable block polyurethane nerve-guidance scaffold enhancing rapid vascularization and promoting reconstruction of transected sciatic nerve in Sprague-Dawley rats

Yuqing Niu<sup>a,\*</sup>, Massimiliano Galluzzi<sup>b</sup>

<sup>a</sup>. Department of Pediatric Surgery, Guangdong Provincial Key Laboratory of Research in Structural Birth Defect Disease, Guangzhou Women and Children's Medical Center, Guangzhou Medical University, Guangzhou 510623, Guangdong, China

<sup>b</sup>. Materials Interfaces Center, Shenzhen Institutes of Advanced Technology, Chinese Academy of Sciences, Shenzhen 518055, Guangdong, China

\*Corresponding authors: Yuqing Niu, niuyuqing@gwcmc.org [+86-020-38076560](tel:+86-020-38076560)

ORCID: NYQ: 0000-0002-9031-7989

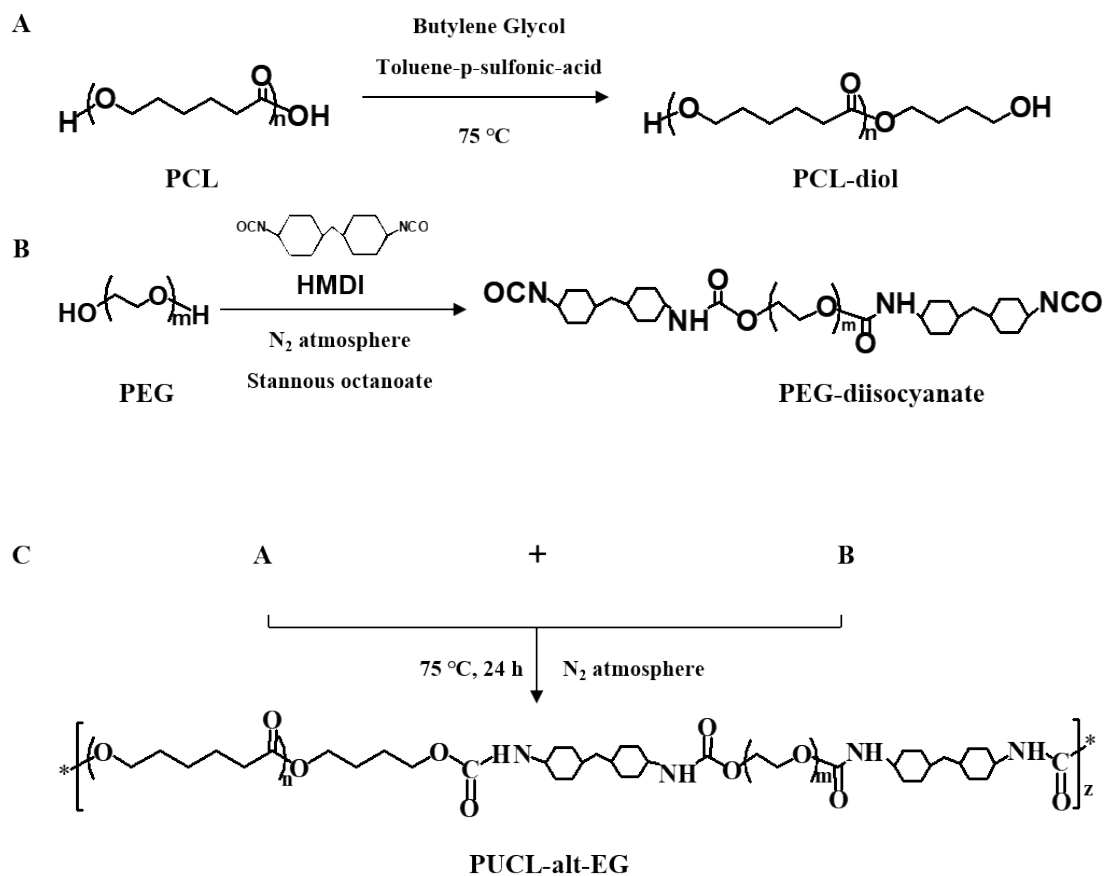


**Fig. S1. Schematic synthesis of the alternating block PU based on PCL-diol and PEG.** Preparation of (A) PCL-diol and (B) PEG-diisocyanate with dihydroxyl terminals; (C) Preparation of the amphiphilic alternating block PU copolymers containing regularly arranged PCL-diol, PEG soft segments and HMDI hard segments.

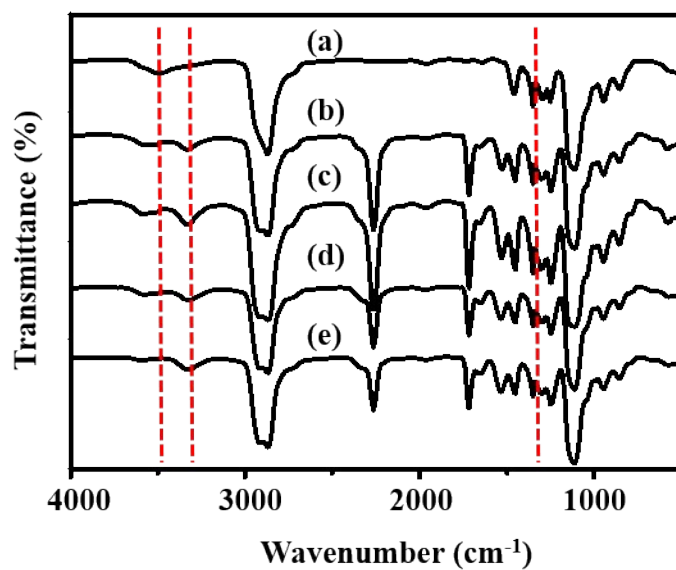


Fig. S2. FTIR spectra of PEG ( $M_n=1000$ ) after reaction with HMDI at different time periods. (a, 0 h; b, 1 h; c, 6 h; d, 12 h; e, 14 h).

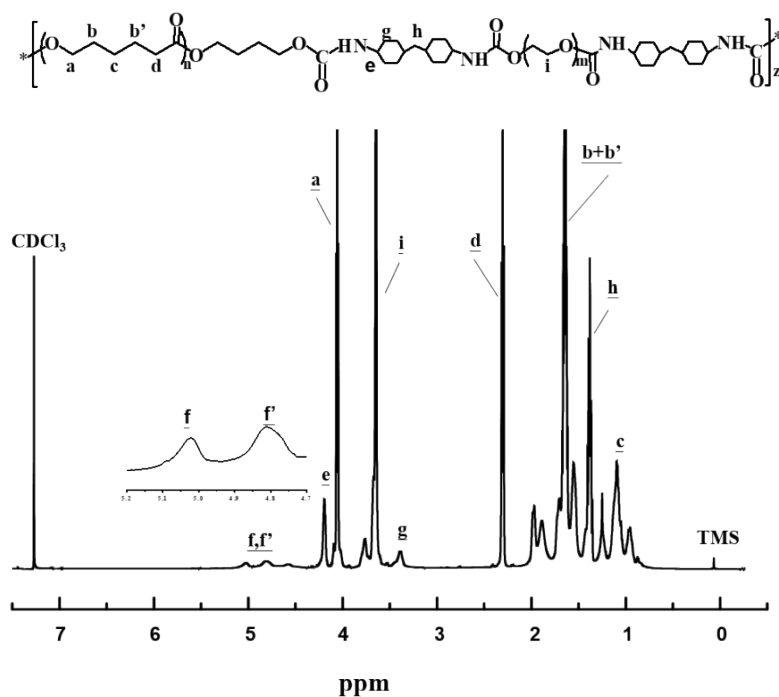


Fig. S3.  $^1\text{H}$  NMR spectrum of alternating block PU copolymer (Table S1) in  $\text{CDCl}_3$ .

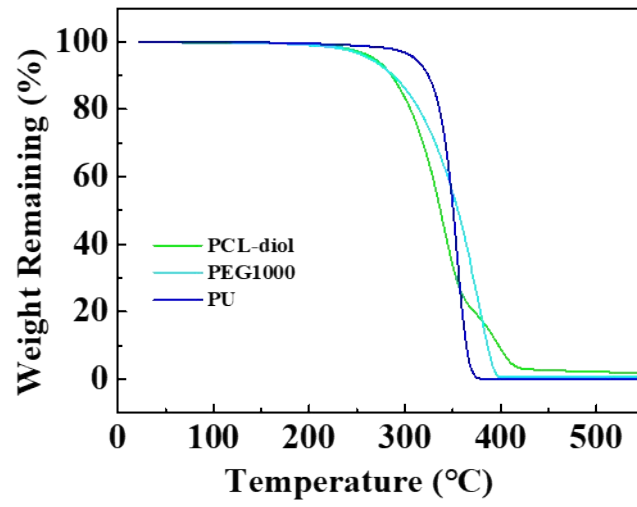


Fig. S4. TGA thermograms of alternating block PU and pre-polymers PCL-diol and PEG.

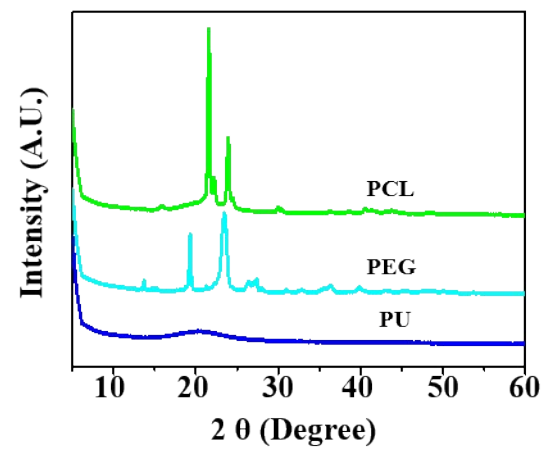
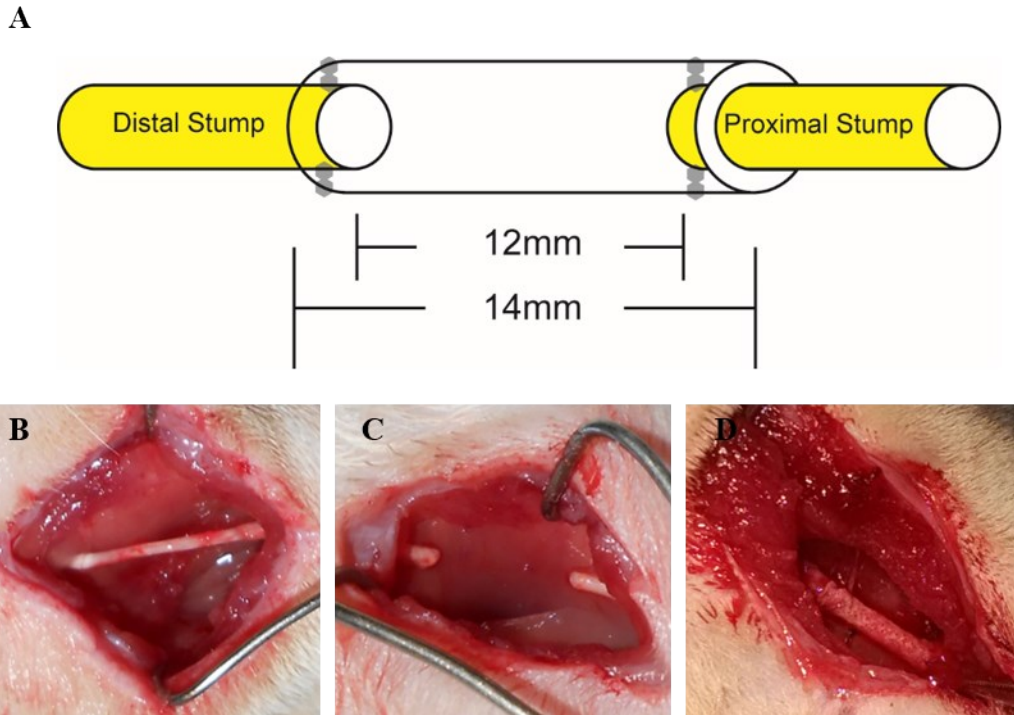
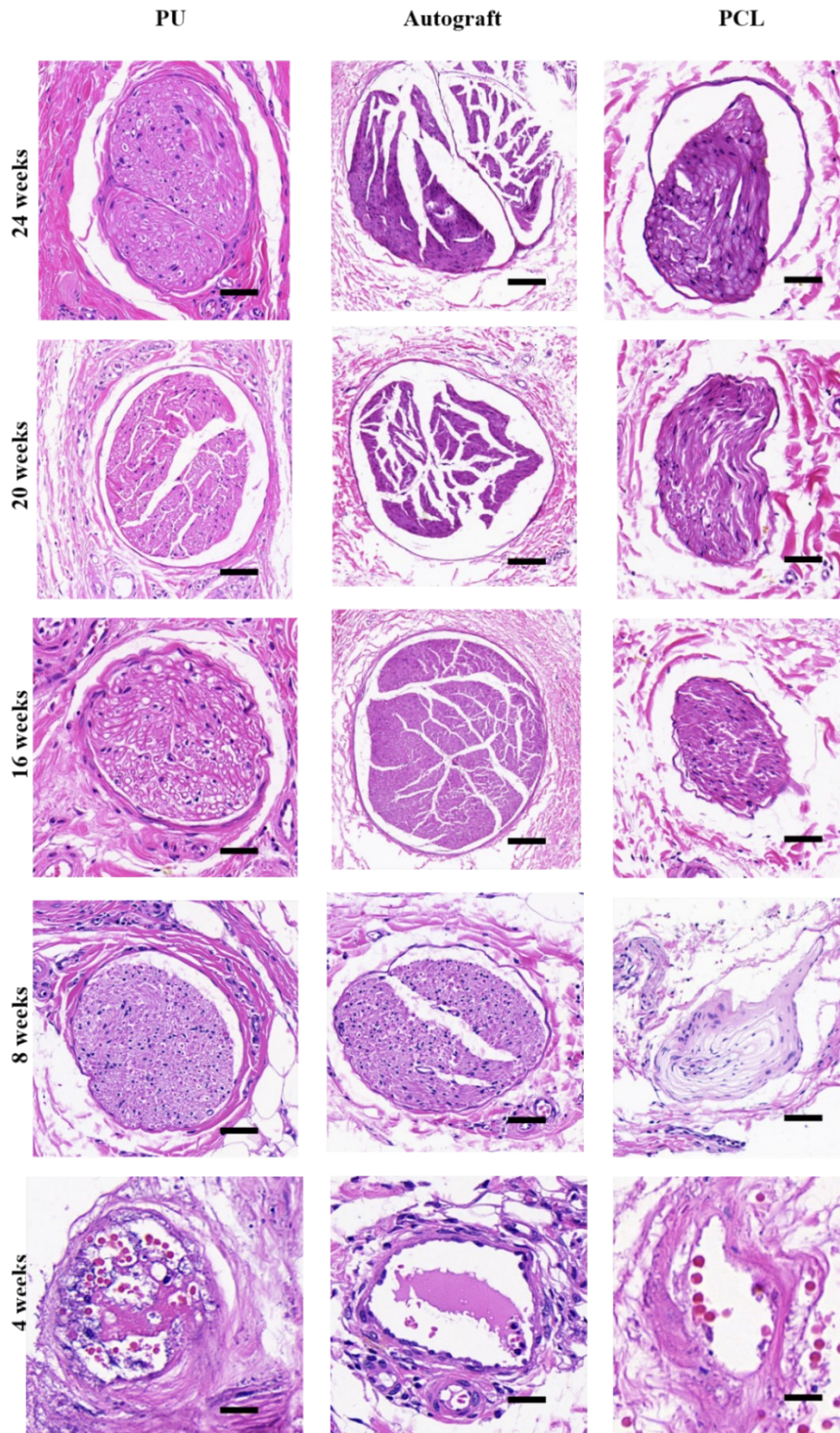


Fig. S5. XRD pattern of the PU, PCL films and PEG powder surface.



**Fig. S6. Overview of the sciatic nerve guidance scaffold PU transplant approach.** (A) A sketch of microsurgery procedure of the 14 mm sciatic nerve guidance scaffold implantation *in vivo*. To create sciatic nerve injury model in SD rats, (B) Localization of sciatic nerve; (C) transection of 12 mm long sciatic nerve; (D) 14 mm PU NGS was bridged between the distal stump and proximal stump.



**Fig. S7.** Histological evaluation of regenerated nerve fibers in the middle cross-section of the graft at the corresponding time points after transplantation. Scale bars, 200  $\mu\text{m}$ .

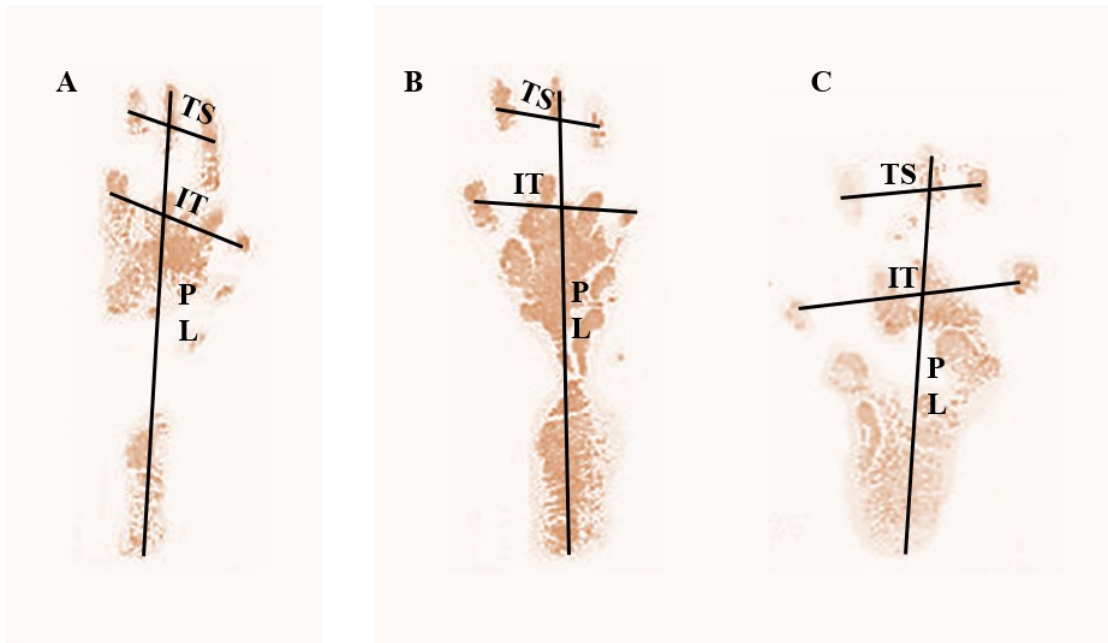


**Fig. S8. Footprint images.** The plantar views of the hind paws of the animals receiving the implantation of PU TENGs at week (A) 4; (B) 8; (C) 16, respectively. The distance between the first and the fifth toes recorded as the parameter "IT", the distance between the third and the fourth toes recorded as the parameter "TS", and the distance between the middle toes to the heel recorded as the parameter "PL".

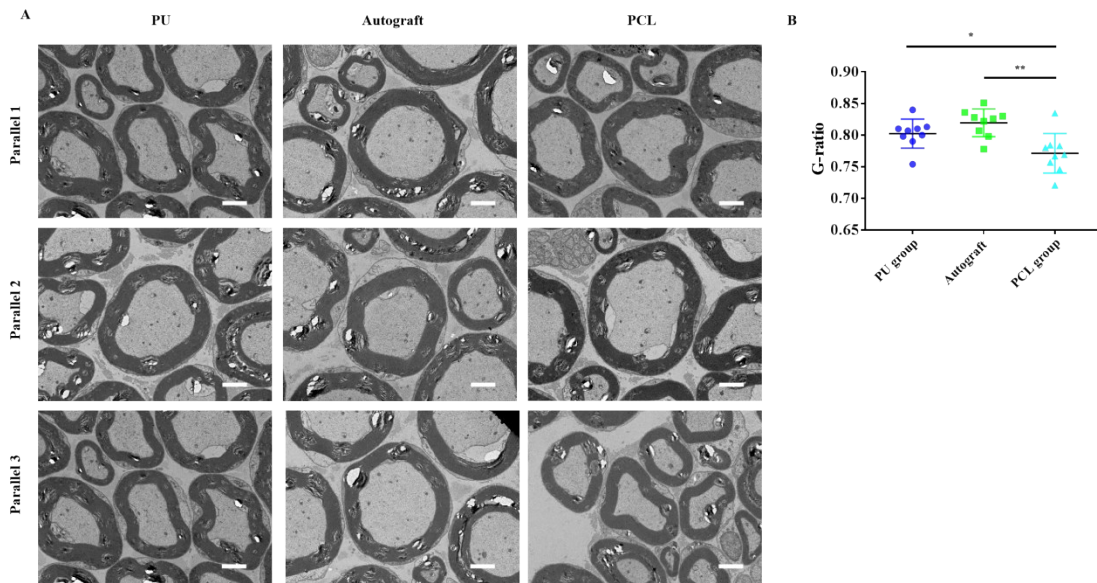


**Fig. S9. Degree of myelination as determined by g-ratio.** (A) TEM micrographs of each group, (B) Mean g-ratios of myelinated axons in each group. (3 images per animal,  $n=3$  animals/group), \* $p < 0.05$ , \*\* $p < 0.01$ . Scale bars, 2.5  $\mu\text{m}$ .

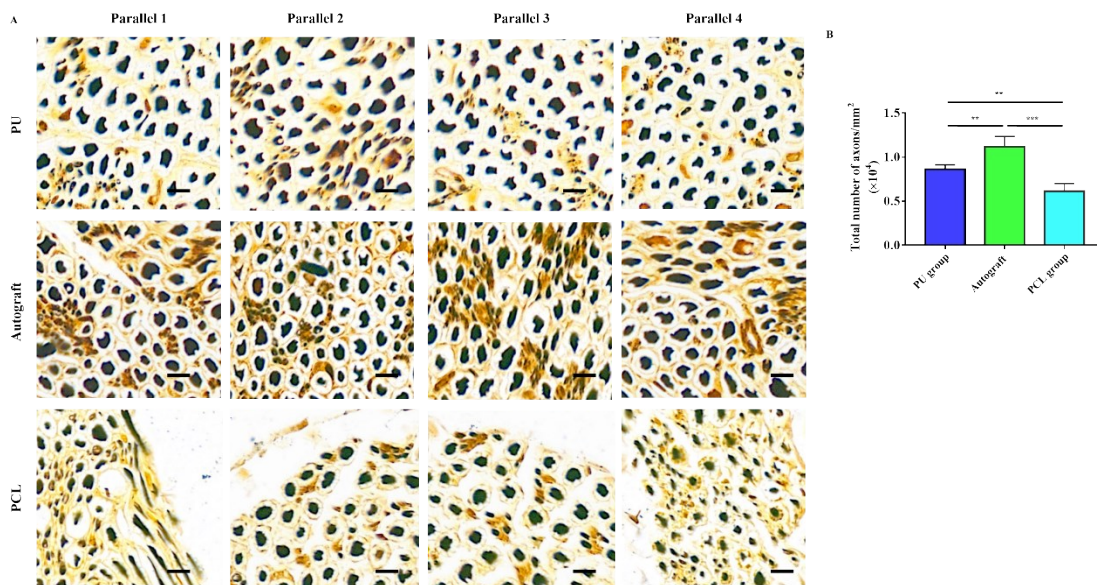


**Fig. S10. Ammoniacal silver staining micrographs and quantification of axons in the middle cross section of the regenerated nerves.** Sections were stained with neurofilament (black, indicating axons). (A) Representative ammoniacal silver staining micrographs in each group. (B) Histograms of myelinated axon densities in each group.  $n = 20$  measurements per sample. \* $p < 0.05$ , \*\* $p < 0.01$ , \*\*\* $p < 0.001$ . Scale bars, 10  $\mu\text{m}$ .

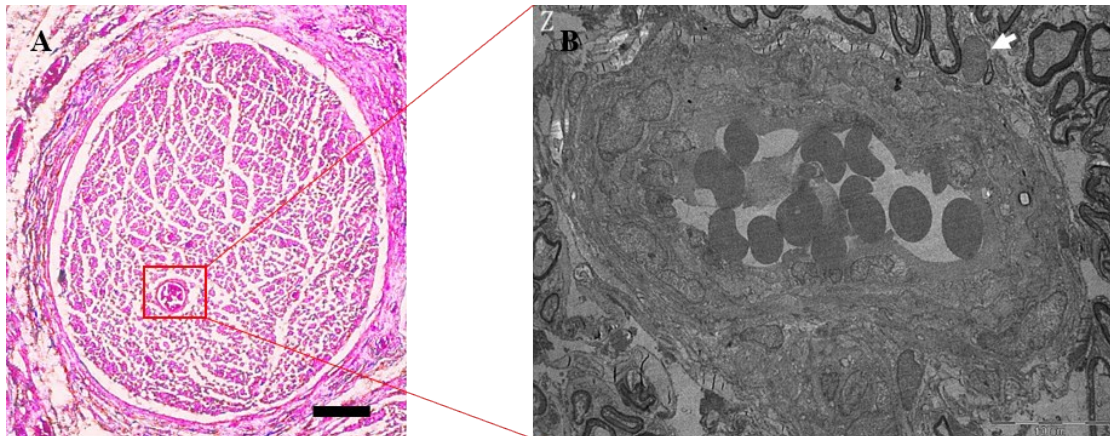


**Fig. S11. Neo-vascularization, nerve fibers and axons within PU NGS after 14 weeks implantation.** (A) HE staining at 4× of the mid-cross section of the PU NGS after 14 weeks implantation. New blood vessels are shown inside regenerated nerve fibers (red box). Scale bar, 500 μm. (B) TEM images revealing the blood vessel structure from the red box of figure A (at 7000 × ). Scale bar, 10 μm.

**Fig. S12. Longitudinal section of regenerated sciatic nerve fibers and axons inside different NGS grafts.** PASM silver staining of longitudinal section of the middle segments regenerated nerve at 14 weeks implantation: (A) PU; (B) autograft; (C) PCL. Scale bars, 20 μm.

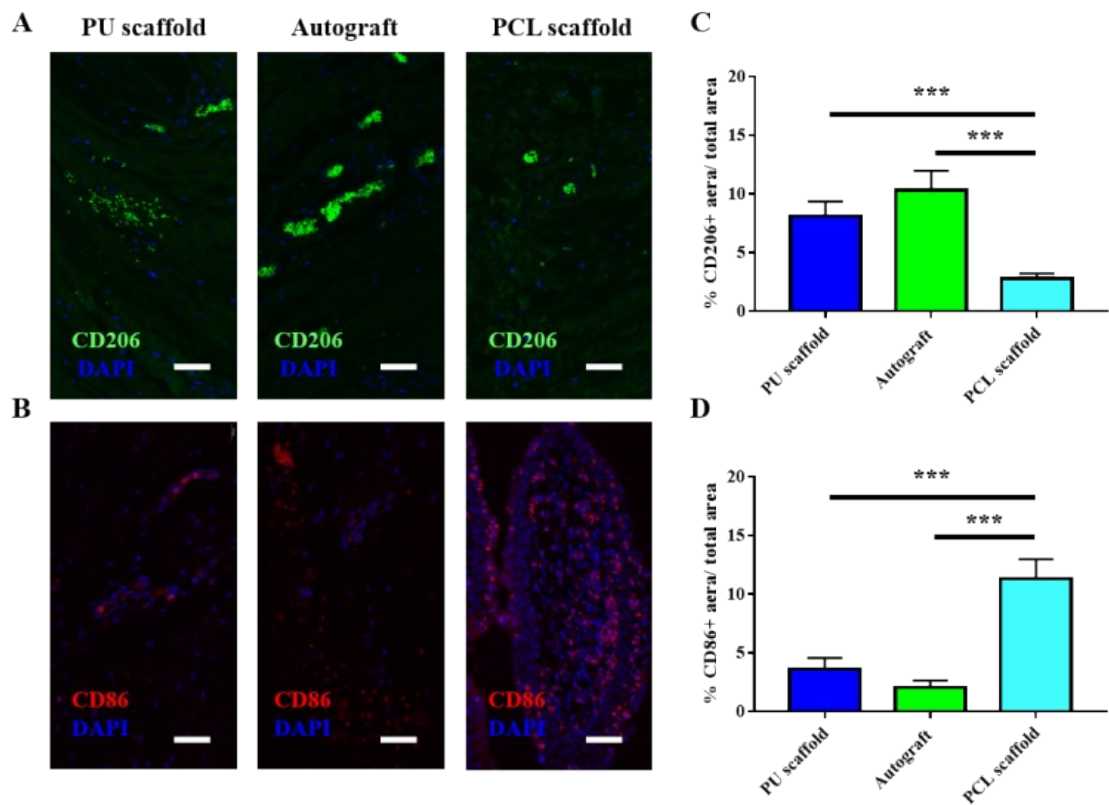


**Fig. S13. Host macrophage response to scaffold at 14 weeks post-implantation.** Fluorescent micrographs of the cross-section of the mid-section of each NGS stained for (A) CD206 (green), nuclei (blue) and (B) CD86 (red), nuclei (blue) 14 weeks post transplantation. Scale bars, 30  $\mu$ m. Quantification of the (C) constructive remodeling M2 (CD206+) macrophages and (D) pro-inflammatory M1 (CD86+) macrophages in each regenerated never ( $n = 3/\text{group}$ ,  $***p < 0.001$ ).

**Table S1. Preparation of PCL and PEG based alternating block polyurethane.**

Sample	R <sup>a</sup>	R' <sup>b</sup>	W <sup>c</sup>	W' <sup>d</sup>	M <sub>w</sub> <sup>e</sup>	PDI <sup>f</sup>
PU	1:2:1	1:2:0.94	47.49	45.14	74800	1.37

<sup>a</sup> R: PCL-diol/HMDI/PEG molar ratio in feed.

<sup>b</sup> R': PCL-diol/HMDI/PEG molar ratio in product calculated from NMR integration.

<sup>c</sup> W: The mass percentage of PEG content in feed.

<sup>d</sup> W: The mass percentage of PEG in product detected by TGA.

<sup>e</sup> M<sub>w</sub>: Determined by GPC in THF.

<sup>f</sup> PDI: M<sub>w</sub>/M<sub>n</sub> determined by GPC using THF as mobile phase.

**Table S2. Contact water angle and mechanical properties of PCL and PU NGS in wet state.**

Sample	θ <sub>H<sub>2</sub>O</sub> (°) <sup>a</sup>	E (MPa) <sup>b</sup>	δ (MPa) <sup>c</sup>	ε (%) <sup>d</sup>
PCL	109 ± 1.5	19.1 ± 0.5	4.8 ± 1.3	120-700
PU	81.5 ± 1.1	30.9 ± 0.3	12.2 ± 0.2	190-1354

a: Contact water angle.

b: Young's modulus.

c: Tensile strength.

d: Strain at break.